Gas-slag-metal equilibrium simulation model of the submerged arc welding process - the effect of flux chemistry on carbon steel weld metal oxygen content

T. Coetsee

University of Pretoria, South Africa

The target level of total ppm O in carbon steel weld metal is 200 ppm to 500 ppm to ensure acceptable weld metal materials properties such as impact toughness. This effect is due to oxide inclusion formation in the weld metal, which may improve or decrease materials properties. Welding fluxes contain a mixture of oxides and fluorides, the latter typically added as CaF_2. Flux formulations are designed in part to control the weld metal total ppm O by using the empirically determined trend of weld metal total ppm O vs. flux basicity (BI) as developed by Tuliani et al. (1969). The application of a gas-slag-metal equilibrium simulation model in the Equilib module of FactSage 7.3 was used to predict the total weld metal ppm O in SAW (Submerged Arc Welding) tests done with different commercial agglomerated fluxes of BI at 0.5 to 3.0. The gas-slag-metal equilibrium results were compared to the chemically analysed weld metal composition values. The model provides improved accuracy in predicted total ppm O values as compared to the empirical trend typically applied in the industry. The model sensitivity is illustrated by incorporating 1-3% $CaCO_3$ in the flux formulation input to the model simulation. The model results with $CaCO_3$ incorporation show up to 50 ppm O increase in weld metal oxygen levels. Therefore, the model flux chemistry inputs must be closely tailored to the flux mineralogy to incorporate such sensitive flux chemistry variations.

INTRODUCTION

Submerged arc welding (SAW) has a long history of development and industrial application, in excess of 100 years (Sengupta *et al*., 2019). SAW is applied in the efficient welding of thick steel plates in heavy engineering industries such as shipbuilding (Sengupta *et al*., 2019). The SAW process is illustrated in cross-section in Figure 1. An electrical current is applied between the weld wire and the steel base plate to form the arc. Raw granular unmelted flux (flux) and molten flux (slag) cover the arc to form the arc cavity. The covered arc ensures high heat transfer efficiency in the arc cavity, compared to higher arc energy losses experienced in open arc welding methods (Sengupta *et al*., 2019). During welding the weld wire and flux are continuously fed through the welding head arrangement as it moves along the weld. Molten weld wire metal droplets are transferred across the arc cavity into the weld pool as complex physical and chemical interactions of heat and mass transfer occur (Sengupta *et al*., 2019). Chemical reactions continue in the trailing molten weld pool of slag and steel until the steel is solidified as weld metal (Chai and Eagar, 1981; Mitra and Eagar, 1991a).

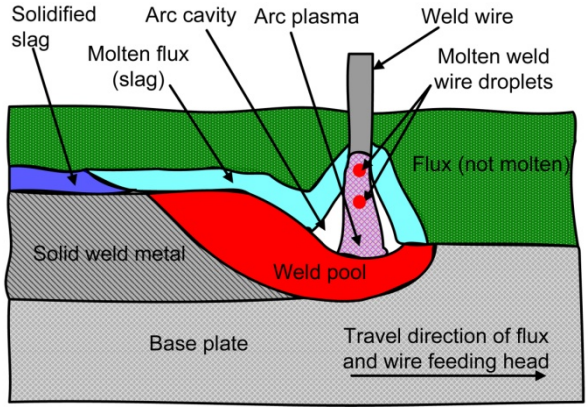

Figure 1. SAW process in cross section.

The welded steel composition is influenced by applied welding parameters of voltage, current, polarity, and welding speed, and by slag-steel-gas chemical reactions in the weld pool and arc cavity (Chai and Eagar, 1981; Mitra and Eagar, 1991a, 1991b, 1991c). Weld pool reaction time is set by heat input, which is itself a combination of voltage, current and welding speed (Kluken and Grong, 1989). Despite the high importance of welding parameters in SAW, the weld metal chemistry is mostly set by the flux composition by controlling of the oxygen potential in the arc cavity (Chai and Eagar, 1980; Mitra and Eagar, 1991b). The flux composition is also formulated to contain source oxides of specific elements for element transfer from the slag to the weld pool for micro-alloying of minor elements such as Ti and B at up to a few hundred ppm (Kohno *et al.*, 1982). For alloying of the weld metal in percentage quantities such as in the case of Mn and Si, the alloying source is typically the weld wire and the flux is formulated to contain oxides of these elements, MnO and SiO_2, to limit alloying element loss to the slag. In addition, the slag must have specific physico-chemical properties to facilitate the SAW process. For example, flux compositions are formulated to ensure optimum levels of slag viscosity and surface tension to sufficiently shield the weld pool from atmospheric gasses; and to ensure that the slag liquidus temperature is typically 50°C lower than the weld metal solidification temperature to ensure easy separation of the post-weld slag from the weld metal surface (Mitra and Eagar, 1991a, 1991c; Singh *et al.*, 2013).

Most SAW fluxes contain fluoride added as CaF_2 to reduce the weld metal hydrogen content by shielding the weld pool from atmospheric air, to increase the slag hydrogen dissolution capacity, and to react with water to form hydrogen fluoride gas (Eagar, 1978; Chai and Eagar, 1982; Burck *et al.*, 1990; Du Plessis *et al.*, 2007; Park *et al.*, 2012). In addition to these reasons for adding CaF_2 to fluxes, the important chemical action of CaF_2 is to lower slag melting temperatures and to serve as a slag network modifier to lower slag viscosity and surface tension. An important empirically determined flux composition guideline is to ensure that the flux basicity index (BI) as expressed in Equation [1], is in excess of 1.5 to ensure low hydrogen and low total oxygen content of 250 ppm O in the weld metal (Tuliani *et al.*, 1969; Eagar, 1978). The aim quantity of total oxygen content in the weld metal of carbon steels is 200 ppm to 500 ppm total oxygen. Both too low (<200 ppm O) and too high (>500 ppm) weld metal oxygen were found to be detrimental to weld metal impact toughness (Dallam *et al.*, 1985).

Equation [1] was originally defined as the ratio of network breaker to network former compounds, each expressed in mass percent, (Eagar, 1978). Equation [1] is an extension of the simple B3 basicity ratio of (%CaO+ %MgO)/($\%SiO_2$) used in pyrometallurgical industry for slags, by adding the compounds typically present in SAW flux.

$$BI = \frac{\%CaF_2+\%CaO+\%MgO+\%BaO+\%SrO+\%Na_2O+\%K_2O+\%Li_2O+0.5(\%MnO+\%FeO)}{\%SiO_2+0.5(\%Al_2O_3+\%TiO_2+\%ZrO_2)} \quad [1]$$

It has been conclusively established that weld metal oxygen originates from the decomposition of flux oxides in arc plasma of the arc cavity (Chai and Eagar, 1982; Lau *et al.*, 1985; Polar *et al.*, 1990). SAW with

binary CaF_2-oxide flux formulations, under Ar atmosphere, confirmed the arc plasma stability order of oxides from high to low stability: CaO, K_2O, Na_2O and TiO_2, Al_2O_3, MgO, SiO_2 and MnO (Chai and Eagar, 1982). Excessive levels of oxygen, beyond the solubility of oxygen in steel, is initially added to the molten weld wire droplets from the arc cavity gas phase, up to 2000-3000 ppm O (Lau *et al.,* 1985; Polar *et al.,* 1990). This initial oxygen level in the metal droplets is sourced from the decomposition of less stable oxides at high temperatures prevailing in the arc cavity, and so flux chemistry is used to manage oxygen transfer to the weld metal from the arc plasma (Indacochea *et al.,* 1985). It was shown that a 100% CaF_2 flux lowers weld metal oxygen since no oxygen is introduced into the weld metal when there are no oxides contained in the flux (Dallam *et al.,* 1985). Similarly, addition of CaF_2 to an oxide containing flux lowers the weld metal total oxygen content as the CaF_2 addition dilutes oxides in the flux (Chai and Eagar, 1982).

In thermodynamic calculations, the level of oxygen available within the weld pool sets the element distribution between slag and metal because of the relative difference in oxygen affinity of the steel alloying elements (Eagar, 1978). Previous studies have shown that the main uncertainty in equilibrium calculations of weld metal compositions is the effect of large quantities of oxygen introduced from the molten flux and gas to the weld pool (Eagar, 1978; Chai and Eagar, 1982; Mitra and Eagar, 1991c). Development of predictive models of the weld metal chemical composition requires a control data set to test the quality of model outputs (Eagar, 1978). Several studies used slag-steel equilibrium calculations as the basis for explaining the effect of flux composition on element transfer between the slag and the weld metal (Palm, 1972; Eagar, 1978; Mitra and Eagar, 1984; Indacochea *et al.,* 1985; Mitra and Eagar, 1991a). Differences between the analysed weld metal composition and the predicted equilibrium values were explained to be due to uncertainty in the accuracy of the equilibrium calculation temperature used to simulate the weld pool reactions, the importance of kinetic factors in reactions, and the importance of the arc plasma reactions in setting slag pool chemistry (Chai and Eagar, 1981; Mitra and Eagar, 1991c). The maximum weld pool temperature reported is 2000 °C (Eagar, 1978; Chai and Eagar, 1981; Mitra and Eagar, 1991a). The maximum temperature at the weld pool-arc plasma interface is estimated as 2500°C (Mitra and Eagar, 1991a, 1991b). An extensive model was developed to account for these effects by incorporating kinetic parameters, slag-metal equilibrium calculations and physical geometric parameters represented by the slag-metal interface area and weld metal volume (Mitra and Eagar, 1991c). However, such a model requires extensive empirical inputs from welding tests. None of these models calculated the weld metal ppm O. Instead, the typical approach was to use empirical data such as the relationship of flux BI vs. ppm O in the weld metal, established by Tuliani *et al.,* (1969), to set the weld metal ppm O level as the input starting point of equilibrium calculations.

This work illustrates the effect of flux chemistry variation on weld metal oxygen content as calculated in the SAW simulation model developed in FactSage 7.3 (Coetsee *et al.,* 2021). The model provides improved accuracy in predicted ppm O values as compared to the empirical trend of Tuliani *et al.,* (1969) as illustrated in comparison of weld metal ppm O to model calculated ppm O from carbon steel weld metal studies (Zhang *et al.,* 2020a, 2020b, 2021).

METHODOLOGY

The accuracy of the simulation model was first evaluated by comparing the model calculated total weld metal ppm O to the total weld metal ppm O analysed in the weld metal samples. Total ppm O refers to the weld metal oxygen content analysed after solidification. A cut of the weld metal cross-section was made by band saw at the centre position of the approximately 30 cm weld run length. The weld metal cross-section sample surface was polished and etched with 2% Nital solution to show the weld metal bead boundary in the base plate. A volume sample was cut from the weld metal using a manual saw. Total ppm O in the weld metal volume sample was determined by combustion method with analysis uncertainty of ±10 ppm O (Coetsee *et al.,* 2021). Calculation of the end-point steel analysis (weld metal) for different flux formulations requires a set of material inputs consisting of flux, wire and base plate chemistries, and their proportions (Coetsee *et al.,* 2021). The welding parameters of voltage, current, and welding speed set the energy input level in the arc cavity and weld pool, and may be represented in the model by the effective chemical reaction equilibrium temperature of 2000°C as specified in previous

studies (Eagar, 1978; Chai and Eagar, 1981; Mitra and Eagar, 1991a). Although higher temperatures may also be considered since the weld pool-arc plasma interface temperature was estimated to be as high as 2500°C (Mitra and Eagar, 1991a, 1991b).

Agglomerated commercial fluxes of wide-ranging basicity index values of 0.5 to 3.0 were selected to produce bead-on-plate welds as described previously (Coetsee *et al.*, 2021). The fluxes were extensively characterised in terms of chemistry and mineralogy as described previously (Coetsee, 2020). The FSstel, FToxid and FactPS databases were selected in the Equilib module (Bale *et. al.*, 2016). Each flux formulation contains different minerals as displayed in Table I. The detailed bulk chemistry of each flux is displayed in Table II. The flux chemistry input to the Equilib model was made in terms of simple oxides, CaF_2 and $CaCO_3$, as is displayed in Table III.

Table I. Mineral phases in commercial agglomerated fluxes (mass%)

Mineralogy phase name	**Flux 1**	**Flux 2**	**Flux 3**	**Flux 4**	**Flux 5**
Fluorite (CaF_2)	36.6	32.0	29.5	21.7	3.2
Corundum (Al_2O_3)	24.6	17.2	16.6	20.2	54.4
Periclase (MgO)	32.8	36.6	41.1	33.3	7.7
Calcite ($CaCO_3$)	0	1.3	3.2	0	0
Wollastonite ($CaSiO_3$)	3.3	8.4	6.1	0	4.4
Mullite ($Al_{4.52}O_{9.74}Si_{1.48}$)	0	0	1.4	17.4	7.3
Quartz (SiO_2)	1.3	1.3	2.1	1.5	2.7
Cristobalite (SiO_2)	0	0	0	1.8	0
Kyanite ($Al_2O_3SiO_2$)	0	0	0	4.1	0
Jacobsite (Fe_2MnO_4)	0	0	0	0	2.2
Manganosite (MnO)	0	0	0	0	1.6
Mn-metal	0	0	0	0	3.1
Zircon ($ZrSiO_4$)	0	0	0	0	4.3
Rutile (TiO_2)	1.3	0.3	0	0	9.1
Forsterite ($Mg_{1.834}Fe_{0.155}Ni_{0.011}SiO_4$)	0	2.9	0	0	0
BI	3.0	1.8	2.9	1.4	0.5

Table II. Bulk chemistry of fluxes (mass%)

Compound	**Flux 1**	**Flux 2**	**Flux 3**	**Flux 4**	**Flux 5**
MnO	0.87	5.83	1.11	6.80	12.30
CaO	24.20	19.90	25.30	12.50	5.27
Al_2O_3	13.90	17.30	17.90	24.90	36.0
SiO_2	15.10	21.30	13.40	19.60	18.60
MgO	32.10	21.20	29.80	22.20	4.94
Fe_2O_3	0.65	1.01	1.10	2.67	5.97
TiO_2	0.74	1.86	1.18	0.97	10.70
ZrO_2	0.01	0.01	0.03	0.02	0.24
Na_2O	2.00	2.69	1.57	1.61	2.20
K_2O	0.78	1.50	1.15	0.18	0.51
P	0.018	0.031	0.015	0.025	0.033
S	0.033	0.028	0.013	0.018	0.020
Cu	0.008	0.008	0.005	0.007	0.011

F	12.5	11.0	12.6	8.41	2.04
Total	102.9	103.7	105.2	99.9	98.8
BI	3.0	1.8	2.9	1.4	0.5

The translation of the bulk chemistry values to that in Table III is based on the stoichiometric allocation of calcium containing compounds $CaCO_3$, CaF_2 and CaO as follows: $CaCO_3$ is taken as the values in Table I from the XRD (X-ray diffraction) analyses, the remaining Ca is then stoichiometrically allocated as CaF_2 based on %F in Table II, and then the last remaining Ca is expressed as CaO. The rest of the elements are expressed as the individual oxides listed in Table III. These different allocations of calcium may seem trivial since relatively low quantities of 1-3 % $CaCO_3$ were identified in fluxes 2 and 3 as shown in Table I. However, the following simulation model results show the effect of $CaCO_3$ content on weld metal ppm O. Also displayed in Table III are the proportions of slag to weld wire melted into the weld pool, and the proportion weld wire in the weld metal (%weld wire in WM). These values were measured from the welding tests and are used as simulation model inputs (Coetsee, 2020).

Table III. Flux composition used as input to FactSage simulation model (mass%)

Oxide/Fluoride	**Flux 1**	**Flux 2**	**Flux 3**	**Flux 4**	**Flux 5**
MnO	0.9	5.9	1.1	7.1	12.6
CaO	5.9	3.0	4.9	0.0	2.3
Al_2O_3	14.3	17.4	17.7	25.9	37.0
SiO_2	15.5	21.4	13.2	20.5	19.2
CaF_2	26.3	22.7	25.6	18.0	4.3
MgO	32.8	21.3	29.4	23.1	5.1
FeO	0.6	0.9	1.0	2.5	5.5
TiO_2	0.8	1.9	1.2	1.0	11.0
ZrO_2	0.0	0.0	0.0	0.0	0.2
Na_2O	2.1	2.7	1.6	1.7	2.3
K_2O	0.8	1.5	1.1	0.2	0.5
$CaCO_3$	0.0	1.3	3.2	0.0	0.0
Total	100.0	100.0	100.0	100.0	100.0
BI	3.0	1.8	2.9	1.4	0.5
gram slag/gram weld wire	0.94	1.02	1.07	0.99	0.89
%Weld wire in weld metal	64	73	64	73	73

In this work the gas-slag-metal equilibrium simulation model calculation is applied to illustrate the sensitivity of model results in terms of minor changes in mineral compound inputs, specifically in terms of the weld metal ppm O. Therefore, an accurate mineral formulation of each flux is an important input to the simulation model.

RESULTS AND DISCUSSION

In Figure 2, the FactSage 7.3 gas-slag-metal equilibrium simulation model calculation values of total oxygen content in the weld metal (ppm O) are compared to the values analysed in the weld metal. Two series of values are shown for the FactSage calculated values, one with $CaCO_3$ included in the input flux composition, and one without. Since only fluxes 2 and 3 contain $CaCO_3$, as shown in the XRD analyses in Table I, the calculated values for these two values are higher by 50 ppm when $CaCO_3$ is included in the input flux composition to the FactSage calculation. The reason for this is that CO_2 released from $CaCO_3$ calcination adds oxygen as CO_2 dissociates to CO and O_2 at the high temperatures prevailing in

the arc cavity (Du Plessis *et al.,* 2007). This effect can be seen from the gas phase compositions and partial oxygen pressure values summarised in Table IV. Especially in the case of flux 3, the partial oxygen pressure is significantly increased from log (Po_2) of -9.1 to -8.1. The concentration of CO in the gas is also increased, and the overall gas volume expressed as gram gas/100 gram flux, is increased from $CaCO_3$ dissociation.

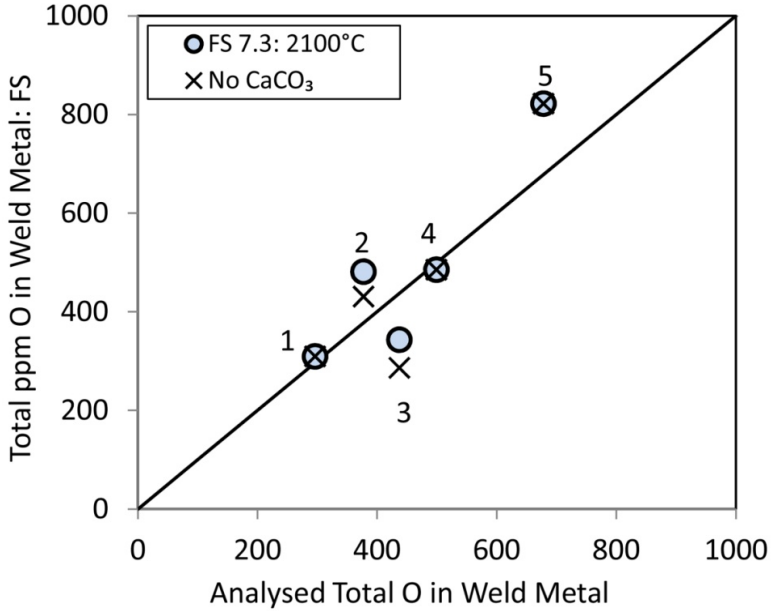

Figure 2. Total weld metal oxygen: FactSage vs. analysed.

*Table IV. Main compounds from FactSage 7.3 gas-slag-metal equilibrium (volume%)**

Flux	**Flux 1**	**Flux 2**	**Flux 2 (+$CaCO_3$)**	**Flux 3**	**Flux 3 (+$CaCO_3$)**	**Flux 4**	**Flux 5**
CO	12	7	12	11	29	9	23
Na	29	8	7	20	14	4	3
K	7	2	2	8	5	<1	<1
Mg	7	1	1	6	4	1	<1
NaF	17	17	17	15	12	11	9
KF	9	10	9	13	10	<1	6
CaF_2	5	13	12	8	8	11	1
MgF_2	6	16	16	8	8	25	1
MgF	3	2	2	4	3	3	<1
AlF_3	<1	5	4	<1	<1	13	12
AlF_2	<1	2	2	1	<1	4	3
$NaAlF_4$	<1	5	4	<1	<1	8	6
TiF_3	<1	1	1	<1	<1	1	18
$KAlF_4$	<1	5	4	1	<1	1	7
gram gas/100	4	11	12	4	6	9	4
log (P_{O_2})	-9.1	-8.3	-8.1	-9.1	-8.8	-8.1	-7.5

*Mn, MnF_2, Fe, SiF_4, SiO, AlF <2%

It has been shown that increased FeO in the post-weld slag correlates to increased weld metal total ppm O (Mitra and Eagar, 1984), as confirmed for this set of experimental results (Coetsee *et al.*, 2021) and shown in Figure 3. The FactSage calculated values also follows this correlation, with increased slag FeO content associated with increased total oxygen content in the weld metal, as is summarised in Table V.

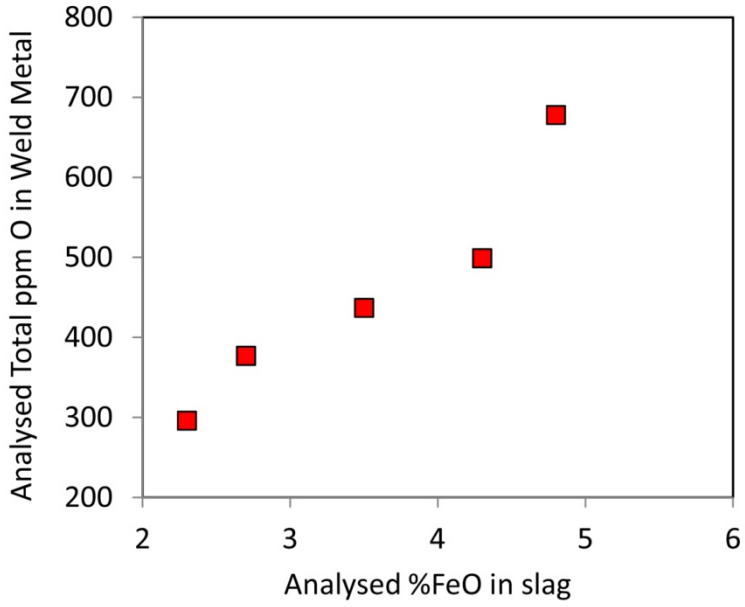

Figure 3. Analysed total weld metal oxygen vs. %FeO in post-weld slag.

Table V. Post-weld slag %FeO and total weld metal oxygen vs. FactSage calculated values

Flux	**Analysed mass% FeO**	**Analysed ppm O**	**FactSage mass% FeO**	**FactSage ppm O**
1	2.3	296	1.9	310
2	2.7	377	2.3	430
2(+$CaCO_3$)	2.7	377	2.6	482
3	3.5	437	2.0	287
3(+$CaCO_3$)	3.5	437	2.8	344
4	4.3	499	2.8	486
5	4.8	678	6.9	822

The FactSage 7.3 gas-slag-metal equilibrium simulation model calculation better corresponds to the analysed total oxygen content values, as compared to the empirical trend from Tuliani *et al.*, (1969) which is typically applied in the welding industry. This is illustrated in Figure 4, also indicating that the trend line of Tuliani *et al.*, (1969) does not provide resolution in the ppm O values at flux basicities beyond 1.8 as it considers a constant value of 250 ppm at higher basicity values. Error bars of the analysed ppm O values are at ± 50 ppm O for indication purposes only, since the analysis uncertainty is ±10 ppm O as stated in the Methodology section.

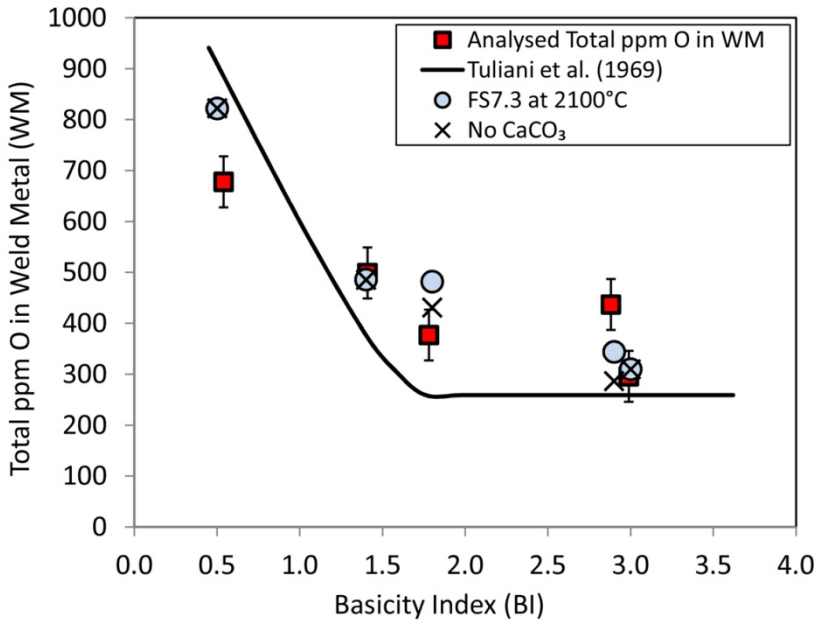

Figure 4. Total weld metal oxygen: FactSage vs. Tuliani et al.*, (1969) trend line vs. analysed.*

Therefore, the FactSage 7.3 gas-slag-metal equilibrium simulation model from this work is an improvement on the existing trendline from Tuliani *et al.,* (1969), and can be used to speed up flux development work by decreasing the amount of physical work required to develop new flux formulations.

CONCLUSIONS

- The FactSage 7.3 gas-slag-metal equilibrium simulation model presented here accurately predicts the weld metal ppm O for different commercial agglomerated fluxes of BI at 0.5 to 3.0 applied in the submerged arc welding of carbon steel.
- This model is a significant improvement from the empirically determined trend line by Tuliani *et al.,* (1969) in terms of improved accuracy in predicted ppm O values, and improved resolution at BI values in excess of 1.8.
- Flux chemistry inputs to the model must be closely tailored to the flux mineralogy to incorporate sensitive flux chemistry variations. This is illustrated here in the sensitivity in the model results when 1-3% $CaCO_3$ is incorporated into the model simulation. The model results with $CaCO_3$ incorporation shows 50 ppm O increase in weld metal total oxygen levels.

ACKNOWLEDGEMENTS

This work was funded by the National Research Foundation of South Africa, grant number BRIC171211293679.

REFERENCES

Bale, C.W., Bélisle, E., Chartrand, P., Decterov, S., Eriksson, G., Gheribi, A.E., Hack, K., Jung, I.-H., Kang, Y.–B., Melançon, J., Pelton, A.D., Petersen, S., Robelin, C., Sangster, J., Spencer, P., and Van Ende, M.–A. 2016. Reprint of: FactSage thermochemical software and databases, 2010–2016. *CALPHAD,* vol. 55, pp. 1–19.

Burck, P.A., Indacochea, J.E., and Olsen, D.L. 1990. Effects of welding flux additions on 4340 steel weld metal composition. *Welding Journal*, vol. 69, pp. 115–122.

Chai, C.S. and Eagar, T.W. 1980. The effect of SAW parameters on weld metal chemistry. *Welding Journal*, vol. 59, pp. 93–98.

Chai, C.S. and Eagar, T.W. 1981. Slag–metal equilibrium during submerged arc welding. *Metallurgical and Materials Transactions B*, vol. 12, pp. 539–547.

Chai, C.S. and Eagar, T.W. 1982. Slag metal reactions in binary CaF_2-metal oxide welding fluxes. *Welding Journal*, vol. 61, pp. 229–232.

Coetsee, T. 2020. Phase chemistry of Submerged Arc Welding (SAW) fluoride based slags. *Journal of Materials Research and Technology*, vol. 9, pp. 9766–9776.

Coetsee, T., Mostert, R.J., Pistorius, P.G.H., and Pistorius, P.C. 2021. The effect of flux chemistry on element transfer in Submerged Arc Welding: Application of thermochemical modelling. *Journal of Materials Research and Technology*, vol. 11, pp. 2021–2036.

Dallam, C.B., Liu, S., and Olson, D.L. 1985. Flux composition dependence of microstructure and toughness of submerged arc HSLA weldments. *Welding Journal*, vol. 64, pp. 140–152.

Du Plessis, J., Du Toit, M., and Pistorius, P.C. 2007. Control of diffusible weld metal hydrogen through flux chemistry modification. *Welding Journal*, vol. 86, pp. 273–280.

Eagar, T.W. 1978. Sources of weld metal oxygen contamination during submerged arc welding. *Welding Journal*, vol. 57, pp. 76–80.

Indacochea, J.E., Blander, M., Christensen, N., and Olson, D.L. 1985. Chemical reactions during submerged arc welding with FeO–MnO–SiO_2 fluxes. *Metallurgical and Materials Transactions B*, vol. 16, pp. 237–245.

Kluken, A.O. and Grong, Ø. 1989. Mechanisms of inclusion formation in Al–Ti–Si–Mn deoxidized steel weld metals. *Metallurgical and Materials Transactions B*, vol. 20, pp. 1335–1349.

Kohno, R., Takamo, T., Mori, N., and Nagano, K. 1982. New fluxes of improved weld metal toughness for HSLA steels. *Welding Journal*, vol. 6, pp. 373-380.

Lau, T., Weatherly, G.C., and Mc Lean, A. 1985. The sources of oxygen and nitrogen contamination in submerged arc welding using CaO-Al_2O_3 based fluxes. *Welding Journal*. vol. 64, pp. 343-347.

Mitra, U. and Eagar, T.W. 1984. Slag metal reactions during submerged arc welding of alloy steels. *Metallurgical and Materials Transactions A*, vol. 15, pp. 217-227.

Mitra, U. and Eagar, T.W. 1991a. Slag-metal reactions during welding: part I. Evaluation and reassessment of existing theories. *Metallurgical and Materials Transactions B*, vol. 22, pp. 65-71.

Mitra, U. and Eagar, T.W. 1991b. Slag–metal reactions during welding: part II. Theory. *Metallurgical and Materials Transactions B*, vol. 22, pp. 73–81.

Mitra, U. and Eagar, T.W. 1991c. Slag-metal reactions during welding: part III. Verification of the theory. *Metallurgical and Materials Transactions B*, vol. 22, pp. 83–100.

Palm, H.J. 1972. How fluxes determine the metallurgical properties of submerged arc welds. *Welding Journal*, vol. 51, pp. 358–360.

Park, J.–Y., Chang, W.–S., and Sohn, I. 2012. Effect of MnO to hydrogen dissolution in CaF_2–CaO–SiO_2 based welding type fluxes. *Science and Technology of Welding and Joining*, vol. 17, pp. 134–140.

Polar, A., Indacochea, J.E., and Blander, M. 1990. Electrochemically generated oxygen contamination in submerged arc welding. *Welding Journal*, vol. 69, pp. 68–74.

Sengupta, V., Havrylov, D., and Mendez, P.F. 2019. Physical phenomena in the weld zone of submerged arc welding - A Review. *Welding Journal*, vol. 98, pp. 283–313.

Singh, B., Khan, Z.A., and Siddiquee, A.N. 2013. Effect of flux composition on element transfer during Submerged Arc Welding (SAW): a literature review. *International Journal of Current Research*, vol. 5, pp. 4181–4186.

Tuliani, S.S., Boniszewski, T., and Eaton, N.F. 1969. Notch toughness of commercial submerged arc weld metal. *Welding and Metal Fabrication*, vol. 37, pp. 327–339.

Zhang, J., Coetsee, T., Basu, S., and Wang, C. 2020a. Impact of gas formation on the transfer of Ti and O from TiO_2-bearing basic fluoride fluxes to submerged arc welded metals: A thermodynamic approach. *CALPHAD*; vol. 71, pp. 102195. https://doi.org/10.1016/j.calphad.2020.102195

Zhang, J., Wang, C., and Coetsee, T. 2020b. Assessment of weld metal composition prediction models geared towards Submerged Arc Welding: case studies involving CaF_2–SiO_2–MnO and CaO–SiO_2–MnO fluxes. *Metallurgical and Materials Transactions B*, vol. 51, pp. 2404–2415.

Zhang, J., Wang, C., and Coetsee, T. 2021. Thermodynamic evaluation of element transfer behaviors for fused CaO–SiO_2–MnO fluxes subject to high heat input Submerged Arc Welding. *Metallurgical and Materials Transactions B*, vol. 52, pp. 1937–1944.

Theresa Coetsee

Senior Lecturer
University of Pretoria

Theresa has 25 years of working experience in the metallurgy industry with mining and metals companies ISCOR, Kumba Resources and Exxaro Resources. At Exxaro Resources she worked as a principal process specialist on the process development of the AlloyStream furnace project for ferromanganese smelting. Since 2016 she is a full-time lecturer at the University of Pretoria in the Department of Materials Science and Metallurgical Engineering.